Simulation of two and three-dimensional disordered systems

Raedt, Hans De; Vries, Pedro de

Published in:
Zeitschrift für Physik. B: Condensed Matter

DOI:
10.1007/BF01313668

Publication date:
1989

Z. Phys. B – Condensed Matter 77, 243–251 (1989)

Condensed
Zeitschrift für Physik B Matter

Simulation of two and three-dimensional disordered systems: Lifshitz tails and localization properties

Hans De Raedt[1, 2, 3] **and Pedro de Vries**[3]

[1] IBM Research Division, Zurich Research Laboratory, Rüschlikon, Switzerland
[2] Physics Department, University of Antwerp, Wilrijk, Belgium
[3] Natuurkundig Laboratorium, University of Amsterdam, Amsterdam, The Netherlands

Received February 16, 1989; revised version May 26, 1989

Very large two and three-dimensional realizations of the Anderson model for localization are studied by solving the time-dependent Schrödinger equation. The density of states is calculated and Lifshitz tails extracted. Eigenstates at various energies are computed and analyzed. The localization length is determined as a function of the strength of the disorder and energy. For moderate disorder substantial deviations from results obtained by the strip-and-rod technique are found.

I. Introduction

The Anderson model for localization is one of the simplest models that describes most of the essential features of electrons in disordered systems. It has been the subject of extensive theoretical studies and observable effects due to localization have been predicted and confronted with experimental data [1–6].

Field-theoretical methods [7, 8], and scaling arguments [9, 10], as well as mode-coupling approximations [11–13], and diagrammatic expansions [14, 15], all show that a particle moving in a two-dimensional (2D) random potential is localized. However, as the strength of the random potential diminishes, the localization length becomes astronomically large so that for all practical (experimental or numerical) purposes the wave function extends over the whole system. For three-dimensional (3D) systems there is a mobility edge and its trajectory in the energy (E/V) – disorder (W/V) plane has been determined (see Ref. 16 for more details and more references).

The most popular numerical method used to study Anderson localization is the strip and rod technique [16, 17–22], combined with finite size scaling analysis yielding results that can be understood in terms of a bound state of a potential well [23]. A crucial step in this iterative method is to extrapolate data of very long strips (rods) of small width (cross section) by means of scaling assumptions.

Numerical simulations for 2D systems, not analyzed with the help of scaling theory, have suggested that there is a critical value, the estimates of the critical disorder being in the range $6 \leqq W/V \leqq 7$ at the band center [24–33]. One finds that there is an abrupt transition from a localized to an extended regime as the degree of disorder decreases. Recently [34] it has been shown that the discrepancy between theory and simulation can be traced back to the fact that the simulations were carried out for systems too small and time-scales much too short to observe localization.

As long as the model system is small one can diagonalize the Hamiltonian numerically. If the emphasis is on Anderson localization, a phenomenon intimately related to the behavior of the wave function at large distances and on long time-scales, only very large systems will exhibit the relevant features. For example, the systems that we deal with in this paper contain typically 60000 to 90000 lattice sites. Matrices of dimension 60000×60000 cannot be diagonalized on present day computers and consequently one has to adopt a different strategy to obtain the physical properties. The equation of motion method introduced by Alben et al. [35] as a method to calculate the (local) density of states (L)DOS of 3D disordered systems is one such technique. By solving the time-dependent Schrödinger equation (TDSE) numerically, information about the spectrum follows directly, without diagonalizing very large matrices.

Although it seems to be a general belief that the TDSE approach is less efficient than those based on the recursion (Lanczos) techniques, it has been argued that this is not necessarily true [36–39]. MacKinnon [36] pointed out that the physical interpretation to the time-development of the wave function is much clearer than that of wave functions generated by recursion methods. An important advantage of the TDSE approach is that once having an accurate solution of the TDSE over an extended period of time, the problem of extracting different physical properties is merely a question of standard data analysis.

Recently it has been demonstrated that the usefulness of the TDSE approach depends critically on the algorithms used to integrate the TDSE [36, 39]. It was shown how to correct for various artifacts resulting from the use of the leap-frog method. The strategy adopted in the present paper is different. Having an accurate, unconditionally stable and very efficient algorithm [34] at our disposal, we only have to focus on the various possibilities to extract and interpret the physical properties that are hidden in the time-dependent wave function.

One aim of this paper is to demonstrate that the TDSE method can effectively be used to calculate different physical properties (some of which are not accessible with other techniques) of very large 2D and 3D random systems. As a model system we will take the standard Anderson model of localization [40], i.e. a tight-binding model (hopping energy V) for a particle that moves in a random potential (uniformly distributed over the interval $[-W/2, W/2]$). An appealing feature of the TDSE method is that it is flexible and not restricted to a specific model, as exemplified in another paper where we discuss its application to the problem of a quantum particle on a 2D fractal network [41]. In particular it will be shown that it can be used to compute the (L)DOS, Lifschitz tails, eigenstates at selected energies, localization lengths, and properties of moving wavepackets.

A second objective of the present paper is to calculate quantities such as the localization length without relying on additional (scaling) assumptions. Our calculations show that for 2D systems in the regime of weak to moderate disorder, the strip method overestimates to considerable extent the localization length. Another notable result [16] of the strip method is that the 2D localization length has its maximum at $E \neq 0$ and not at $E=0$ as one might expect. Our calculations do not support this finding.

In Chap. II we present details about the technique used to extract from the solution of the TDSE information about the physical properties of interest. Chapter III reviews our results for the density of states. The Lifshitz tails are treated in Chap. IV. Chapter V discusses the results of the analysis of the spatial behavior of the eigenstates and compares our findings for the localization length with previous work. The effect of disorder on the 3D motion of a quantum particle in the regime where extended states exist is also examined in Chap. V.

II. Method

The basic idea is to solve the TDSE ($\hbar = 1$)

$$\frac{\partial \psi(\mathbf{r}, t)}{\partial t} = -\mathrm{i} H \psi(\mathbf{r}, t), \tag{2.1}$$

for a particle moving on a square or cubic lattice and feeling a random potential. In general the TDSE approach entails three steps:

a) Set up the initial state, i.e. the wave function at $t=0$.

b) Solve the TDSE.

c) Analyze the data.

As all details of step *b)* have been extensively discussed elsewhere [34] we will not expand on it here. The choice of the initial state is important because it determines to a considerable extent the kind of information that one can extract from the time-development of the wave function. Consequently it is difficult to disentangle the discussion of steps *a)* and *c)*.

Conceptually the simplest thing one can do is to let the particle start at a particular lattice site, preferably near the center of the lattice. As time goes on the probability on the other lattice sites will grow. There are two possibilities. If, after some time, the probability on the lattice boundary becomes appreciable, one should stop the calculation unless one is interested in boundary effects themselves. Otherwise the particle is effectively confined to a finite region of space containing the point where it started. Clearly this type of setup is the most direct numerical realization of Anderson's original description of the concept of localization [40]. The relevant quantity is the return probability [40] defined by

$$p(t) \equiv |\langle \phi | \, \mathrm{e}^{-\mathrm{i}Ht} | \phi \rangle|^2, \tag{2.2}$$

where ϕ is the initial state. Our calculations show that the return probability is very noisy and difficult to interpret quantitatively. Therefore we will not dis-

cuss it any further. An important physical quantity is the density of states on ϕ defined by

$$n_\phi(E) \equiv -\frac{1}{\pi} \lim_{\varepsilon \to 0} \mathrm{Im} \langle \phi | (E + i\varepsilon - H)^{-1} | \phi \rangle, \tag{2.3a}$$

$$= \frac{1}{2\pi} \int_{-\infty}^{+\infty} dt e^{iEt} \langle \phi | e^{-itH} | \phi \rangle. \tag{2.3b}$$

The LDOS for a certain lattice site is obtained by choosing ϕ such that it is zero everywhere except on that lattice site. To compute the global DOS, defined as

$$n(E) \equiv \frac{1}{2\pi} \int_{-\infty}^{+\infty} dt e^{iEt} \mathbf{T} r e^{-itH}, \tag{2.4}$$

one can simply average several LDOS. As the number of LDOS is equal to the number of sites, some sampling procedure is necessary if the number of lattice sites is large. A more efficient way is to choose the ϕ's as random functions of the position [36, 42]. In practice it turns out that taking one to ten of such ϕ's is sufficient to get accurate results.

As in any numerical calculation the number of sites as well as the number of points in time used to compute the Fourier transform is finite, the LDOS will consist of a number of sharp spikes, the position of which gives an estimate for an eigenvalue of H, corresponding to an eigenstate which has a nonzero overlap with the initial state. Having determined the eigenvalues, it is also possible to compute the corresponding eigenstates *without* diagonalizing the Hamiltonian [43]. Suppose that in the course of solving the TDSE for an initial state ϕ, we compute

$$|\psi(E)\rangle \equiv \frac{1}{2\pi} \int_{-\infty}^{+\infty} dt e^{iEt} e^{-iHt} |\phi\rangle. \tag{2.5}$$

Upon expanding ϕ in eigenstates of H (i.e. $H\phi_k = E_k \phi_k$) it follows that

$$\lim_{E \to E_k} |\psi(E)\rangle = |\phi_k\rangle \langle \phi_k | \phi \rangle, \tag{2.6}$$

assuming ϕ_k to be non-degenerate. Thus it is possible to calculate the eigenstate corresponding to the eigenvalue E_k provided the estimator E is close to an eigenvalue of H and the overlap $\langle \phi_k | \phi \rangle \neq 0$. The latter can actually be used to "tune" the method. For instance, if we do not want surface states to interfere we take ϕ such that it is nonzero close to the center of the lattice and zero otherwise. In this manner the overlap with surface states will be very small if the lattice is sufficiently large.

To implement this idea one proceeds as follows. For a particular choice of ϕ one solves the TDSE and determines the LDOS. The LDOS provides estimates for the eigenvalues. One then makes an identical, second run but in addition one also computes (2.6) for a few of the eigenvalues found in the LDOS. A definite advantage of this scheme is that in practice one only needs storage for as many eigenstates as one would like to calculate.

It remains to be specified how we handle the problem of performing the Fourier transforms in (2.4) and (2.6). Noting that the real (imaginary) part of the wave function is even (odd) in time we have, in practice,

$$|\phi(E)\rangle \equiv \frac{1}{2\pi} \int_{-\infty}^{+\infty} dt e^{iEt} e^{-iHt} |\phi\rangle, \tag{2.7a}$$

$$\approx \frac{1}{\pi} \int_0^T dt\, w(t) [\mathrm{Re}(|\phi(t)\rangle) \cdot \cos Et - \mathrm{Im}(|\phi(t)\rangle) \sin Et], \tag{2.7b}$$

where T denotes the time up to which the TDSE was solved and $w(t)$ represents a suitable window to compensate for the fact that T is finite. Our experience has shown that the modified Hanning window $w(t) = [1 + \cos(\pi t/T)]/2$ is superior to other simple windows such as the exponential, Gaussian, Hanning etc. To compute the LDOS or DOS we convert (2.7) into a form suitable for the Fast Fourier Transform (FFT) by doubling the interval of integration, exploiting the symmetry of the real and imaginary part of the time-dependent wave function. This procedure becomes impractical when we want to compute the Fourier transform of the wave function itself because that would require storing the wave function at each time step. Consequently we perform the integral (2.7) during the integration of the TDSE.

To maximize the efficiency of such calculations, the time-step τ used to sample the time dependent wave function and the time-interval T have to be chosen judiciously. As the spectrum of the Anderson model lies in the interval [44] $[-(2d|V| + |W|/2), 2d|V| + |W|/2]$ where d is the dimensionality of the lattice, there is no reason to compute the Fourier transform for energies not in the range. This means that τ should satisfy

$$\tau \leqq \frac{4\pi}{4d|V| + |W|}. \tag{2.8}$$

In practice it turns out that for all cases of interest, integration of the TDSE employing the fourth-order method introduced in Ref. 34 and using a time-step equal to τ as given by (2.8) yields very accurate results

Table 1. Asymptotic behavior of the second moment of $|\psi(\mathbf{r}, t)|^2$, the probability of finding the particle at point $\mathbf{r}$ at time t for the different cases of interest. The dimensionality of the system, the linear size, the diffusion constant, the localization length and the fractal dimension are denoted by d, L, D, and ξ respectively

	Wave Function	$\langle \mathbf{r}^2(t)\rangle - \langle \mathbf{r}(t)\rangle^2$
Uniform	$\lvert\psi(\mathbf{r}, t)\rvert^2 \propto L^{-d}$	$d(L^2-1)/12$
Extended	$\psi(\mathbf{r}, t) \propto e^{-i\mathbf{k}\cdot\mathbf{r}}$	t^2
Diffusion	$\frac{\partial}{\partial t}\lvert\psi(\mathbf{r}, t)\rvert^2 = D\Delta\lvert\psi(\mathbf{r}, t)\rvert^2$	$2dDt$
Localization	$\lvert\psi(\mathbf{r}, t)\rvert^2 \propto e^{-r/\xi}$	$d(d+1)\,\xi^2$

for the time dependent wave function. The resolution in energy ΔE is determined by T, i.e.

$$\Delta E = \frac{\pi}{T}, \tag{2.9}$$

whereby use has been made of the symmetry $t \to -t$ mentioned earlier.

Information about the nature of the quantum motion can be obtained by looking at the time dependence of the moments of the wave packet defined as

$$\langle \mathbf{r}^n(t)\rangle \equiv \langle \phi |\, e^{iHt}\mathbf{r}^n e^{-iHt}\,|\phi\rangle, \tag{2.10}$$

where ϕ stands for the initial state. In Table 1, the time dependence of the second (central) moment is given for some of the most common situations. The time-dependent behavior of this quantity as observed during the solution of the TDSE will enable us to classify the kind of motion the quantum particle makes. Higher moments can then be used to test a specific hypothesis in more detail. For instance if the second moment settles to a constant value as time goes on, the particle is localized in space, unless the probability on the lattice boundary is substantial. Assuming exponential decay of the wave function, i.e. $\psi(\mathbf{R}) \propto e^{-R/2\xi}$ for large $\mathbf{R}$ where $\mathbf{R}$ denotes the distance from the center of wave function (as given by $\langle \mathbf{r}\rangle$), the localization length ξ readily follows from the appropriate expression given in Table 1. Similarly, the localization length can also be estimated from the probability distribution "integrated" over one (or two in 3D) directions [29, 41]. The hypothesis of exponential decay can partially be tested by computing the same localization length from the fourth moment. More sophisticated procedures for analyzing the spatial dependence require the calculation of projections of correlations $\psi^*(\mathbf{r}, t)\,\psi(\mathbf{r}+\mathbf{r}', t)$ [41]. For the present purposes there seem to be no need to invoke such techniques. Evidently these kinds of analyses can also be applied to the eigenstates obtained from the procedure outlined above. Another, frequently used, quantity that signals the transition from extended to localized motion is the inverse participation ratio (IPR) [25, 26, 29, 42, 45]. Our calculations show that as a function of time, the noise on this quantity is larger than on the moments. Consequently we have not used it for quantitative work.

Before turning to the discussion of the results, a comment on the choice of the boundary conditions used in the simulations is in order. Usually periodic boundary conditions are chosen to mimic the infinitely large system as well as possible. For problems related to localization this is not the most appropriate choice as it effectively halves the length-scale over which the wave function can be studied, leading to spurious effects in some cases [34, 46]. The simulation results reported below have been obtained using free boundary conditions, i.e. wave packets incident on lattice boundaries are being reflected.

III. Density of states

If the random potential is not present, the infinite system is translational invariant and the DOS can be calculated analytically [47]. For a large lattice it is expected that the LDOS for a particle put at the center of the lattice will closely resemble the DOS of the infinite system. Figure 1 shows that for a 209×209 lattice this is indeed the case. Minor differences appear at the band center $E=0$ and at the band edges $E=4|V|$. For a free particle on an infinite square lattice $n(E) \propto \ln(E)$ for $E \to 0$ [47]. As in practice the time-interval $[-T, T]$ entering the Fourier transform is finite, such a weak divergence is difficult to reproduce numerically. However this is not a point of concern when disorder is present. Indeed it has been shown [44] that $n(E) \leqq 1/|W|$ if $W \neq 0$, and hence the DOS of the Anderson model is always finite. The exact 2D DOS is discontinuous at the band edges $E=4|V|$, [47] whereas numerically the jumps are rounded somewhat. This is due to the finite-E resolu-

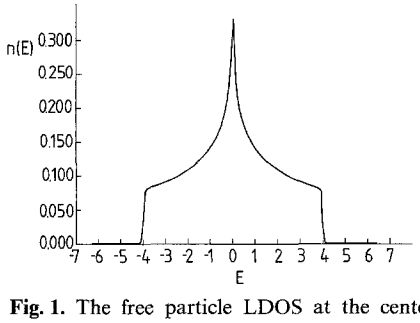

Fig. 1. The free particle LDOS at the center of a square lattice of 209×209 sites. Energy E is in units of the hopping energy V

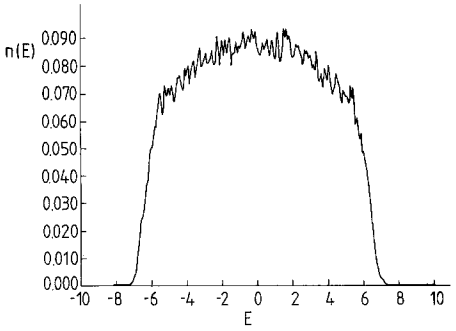

Fig. 2. Average of 10 LDOS on random states for the case of a strongly disordered ($W=10V$, all states localized) 209×209 site lattice. Fluctuations are statistical noise due to the randomness in the participating states. Energy E is in units of the hopping energy V

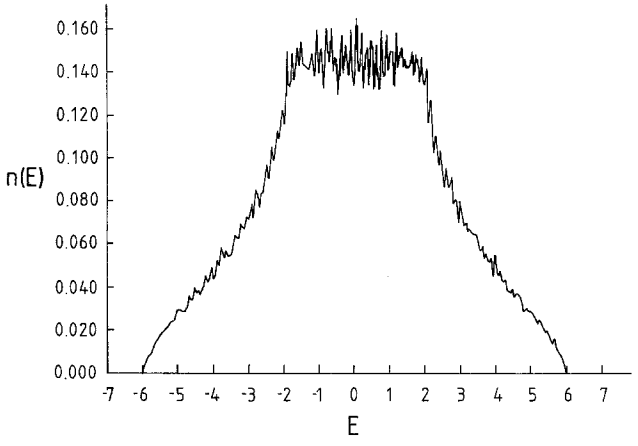

Fig. 3. The free particle LDOS on one random state for a simple cubic lattice of $41 \times 41 \times 41$ sites. Energy E is in units of the hopping energy V

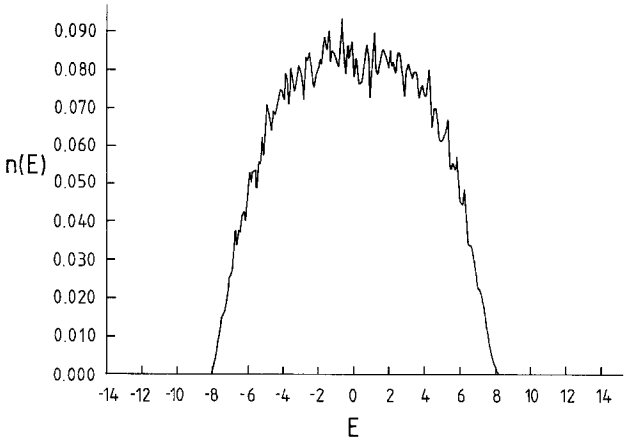

Fig. 4. Average of 10 LDOS on random states for the case of a moderately disordered ($W=10V$, not all states localized) $41 \times 41 \times 41$ site lattice. Energy E is in units of the hopping energy V

tion or, in other words, also due to the finite value of T. The precise form of $n(E)$ at the band edge is determined by the choice of the window $w(t)$. This rounding effect should be taken into account when one wants to examine the tails of the spectrum of a disordered system.

The DOS, obtained by averaging 10 LDOS, for a 2D strongly disordered ($W=10V$) system is depicted in Fig. 2. To compute each LDOS an initial state ϕ was generated randomly over the whole lattice, using a Gaussian envelope chosen such that the probability is concentrated around the center of the lattice and excluding surface states as much as possible. Typically in our calculations, one quarter of the lattice site participates in the averaging process, the fluctuations being proportional to $N^{-1/2}$ where N is the number of sites that participate. Note that the numerical results of Fig. 2 satisfy the rigorous bound [44].

The free particle LDOS for a 68921-site simple cubic lattice on *one* random ϕ is given in Fig. 3. Apart from some noise reflecting the randomness in ϕ, $n_\phi(E)$ is close to the exact 3D DOS [47]. Averaging 10 LDOS of a 3D disordered ($W=10V$) system yields the DOS shown in Fig. 4. Again the rigorous bound [44] is satisfied. Note that in 3D $W=10V$ corresponds to a case where both extended states and localized states coexist [16] whereas in 2D all states are localized. Comparison of Fig. 2 and Fig. 4 shows that in 2D and 3D, DOS do not differ in any significant respect, as expected [1].

IV. Lifshitz tails

Explanations for the Urbach tails in optical absorptions near band edges (i.e. $\ln\alpha(E) \propto E + c$ where α, E, and c denote the absorption coefficient, the energy and a constant respectively) have linked the presence of exponential tails in $\alpha(E)$ to that of the presence of Lifshitz tails in the DOS [48, 49]. General theory [48–51] predicts that $\ln n(E) \propto E^n$ with $1/2 \leqq n \leqq 2$ depending on the energy and range of correlation of the disorder. To keep the mathematics manageable theoretical derivations heavily rely on the assumption that the probability distribution of the random potential is Gaussian. On the other hand it is well-known that band tails resulting from disorder can change significantly if the probability distribution of the random potential is altered [48, 49]. To address the general nature of the relationship between the Urbach tails and tails in the DOS, it is therefore of interest to calculate without approximations the Lifshitz tail for a case where the probability distribution $P(V(\mathbf{r}))$ of the random potential has a finite instead of an

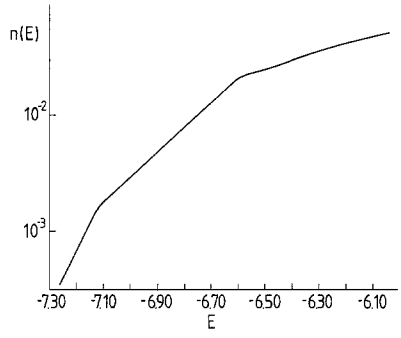

Fig. 5. Tail of the DOS of a strongly disordered ($W=10V$, all states localized) 301×301 site lattice. For $-7.1\leqq E\leqq-6.5$ the Lifshitz tail appears. Energy E is in units of the hopping energy V

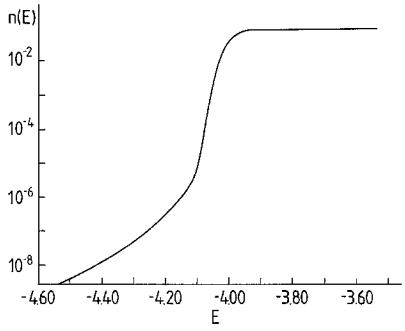

Fig. 6. Tail of the DOS for the free particle case ($W=0$) showing how the finite time interval used in the simulation affects the tail of the spectrum, thereby demonstrating that the main features of Fig. 5 cannot be attributed to finite-time artifacts. Energy E is in units of the hopping energy V

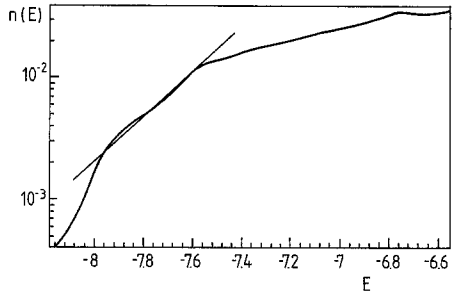

Fig. 7. Tail of the DOS of a moderately disordered ($W=10V$, not all states localized) $41\times41\times41$ site lattice, showing the presence of a Lifshitz tail. Energy E is in units of the hopping energy V

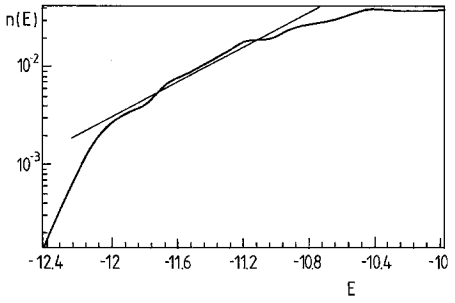

Fig. 8. Tail of the DOS of a strongly disordered ($W=20V$, all states localized) $41\times41\times41$ site lattice, showing the presence of a Lifshitz tail. The energy interval over which the Lifshitz tail appears is approximately twice as large as in Fig. 7. Energy E is in units of the hopping energy V

infinite support. This is the case for the Anderson model where $P(V(\mathbf{r}))=1/(2|W|)$ if $-|W|/2\leqq V(\mathbf{r})\leqq|W|/2$ and $P(V(\mathbf{r}))=0$ otherwise. In addition the range of correlation on the potential is very short, i.e. on-site only. To our knowledge the calculations presented here are the first to yield quantitative results on the Lifshitz tails of the Anderson model.

The simulation result for the tail of a 2D strongly disordered ($W=10V$) system containing 90601 sites is shown in Fig. 5. In this case the energy interval for which $\ln n(E)\propto E$ is appreciable. To rule out that what is seen in Fig. 5 is due to the numerical procedure used, the corresponding result for the free particle case ($W=0$) is given in Fig. 6. It is easy to check that the particular window function employed in the Fourier transform procedure can modify the tail by a factor of $\mathcal{O}(E^{-1})$, an effect which is much too small to be seen on the semi-log scale. Following Ref. 48, the tail observed in Fig. 5 may be identified as a Lifshitz tail. Efforts to identify the Halperin-Lax or Gaussian region [49] have failed.

Some results for the tails of the DOS of 3D systems of 68921 sites are shown in Fig. 7 and Fig. 8. In the former one ($W=10V$) there are both extended and localized states [16], whereas according to recent estimates [16, 21, 52], the latter one ($W=20V$) should have localized states only. Clearly Figs. 7 and 8 do not differ qualitatively, as expected [1]. The regime for which $\ln n(E)\propto E$ is, in both cases, a fairly large fraction of the full bandwidth. In general our results show that for the Anderson model $\ln n(E)\propto E$, supporting the idea [48] that for any disorder having a length scale of the lattice spacing $\ln n(E)\propto E^n$ with $n=1$.

V. Localization length

In Chap. II we discussed various possibilities to extract information about the decay of the (envelope) of the wave function as a function of the distance. In this section we present 2D and 3D results obtained by calculating the second and fourth central moment of eigenstates of different energies. As explained above, these eigenstates are calculated from the time-

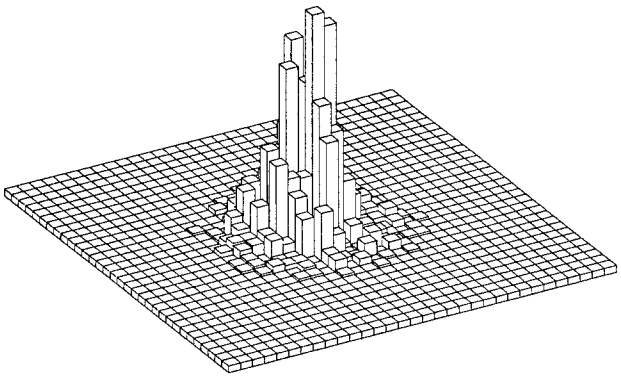

Fig. 9. The "coarse grained" picture of the most extended (localized) eigenstate on a moderately disordered ($W=5V$) 301×301 square lattice

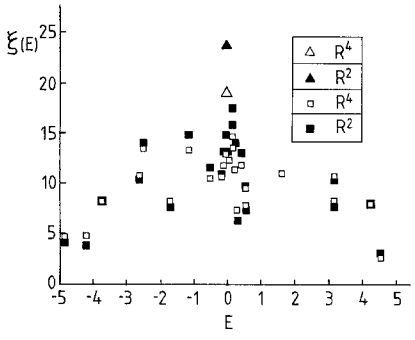

Fig. 10. The 2D localization length $\xi(E)$ for $W=5V$ of eigenstates of different energies E, obtained from the second (solid squares) and fourth (open squares) moment. Also shown are the results (second moment: solid triangle, fourth moment: open triangle) of the typical wave packet comprising some of the eigenstates. Energy E is in units of the hopping energy V

development of a wave packet. Asymptotically, the wave packet will also be localized if all eigenstates that contribute to it are localized. Moreover each of the eigenstates does not necessarily have the same "center of localization," i.e. not the same first moment. This implies that localization length determined from wave-packet itself will be a rather complicated function of the localization length of the eigenstates. In general the localization length obtained from the wave-packet will be larger than that of its constituents and different if one uses different moments.

To test the unexpected result [16] of the strip method that the 2D localization length has its maximum at $E\neq0$ (according to Ref. 16, for $W=5V$ the maximum occurs at $|E|\approx2V$) and not at $E=0$ we calculated many eigenstates for several square lattices of 90601 sites and $W=5V$. A course-grained picture of the most extended eigenstate found is given in Fig. 9. Clearly it is localized in space. All our data for the localization length for $W=5V$ are presented in Fig. 10. A first observation is that for a fixed energy

Table 2. Comparison of the TDSE results for the largest localization length for ($E=0$) of the 2D Anderson model with those obtained by the strip technique [21] and potential-well analogy [23]. The factor 2 in $\lambda\equiv2\xi$ stems from a slightly different definition of the localization length

W	λ (present)	λ (Ref. 21)	λ (Ref. 23)
5	36	97.58	147
6	32	37.46	41.26
10	5.4	5.45	5.34

E, the localization length can easily change by a factor of two, probably because of big differences in the local environment. Such large fluctuations have been found in exact diagonalizations [29] too, although for this particular value of the disorder $W=5V$, the system used in the diagonalization work was too small to support states with a large localization length. Taking these statistical fluctuations into account there is a clear trend that the localization length reaches its maximum at $E=0$, in disagreement with Ref. 16. Our data for $W=6V$ and $W=10V$ (not shown) lead to the same conclusion. Also shown in Fig. 10 are values for the localization length obtained from the fourth central moment. If the eigenstate decays exponentially at large distances they should agree with those calculated from the second moment. In the majority of cases they do but in some disagreement cannot be attributed to statistical noise. If both values differ the one obtained from the second moment is found to be the largest, implying that the eigenstate decays *more quickly* than exponentially.

Table 2 contains some results for the largest localization length, as obtained by three methods. The method [23] used to calculate the numbers of the fourth column is not entirely independent of that used for column three [21]. The general trend is that the strip method seems to overestimate the value of the localization length, especially when the disorder decreases. This may be due to the fact that this technique takes averages over many eigenstates, a procedure which has some similarity to the one that extracts the localization length from a wave packet comprising many eigenstates. Results obtained from the full wave packet are given in Ref. 34 and confirm that the localization length of the wave packet is larger than that of the eigenstates. Also the strip method becomes less accurate as the disorder becomes smaller [16].

There is considerable discrepancy, even on a qualitative level, between the results of Ref. 33 and ours. It has been shown [34] that this is readily traced back to the fact that the simulations of Ref. 33 have been carried out using lattices and time intervals too small to see localization set in.

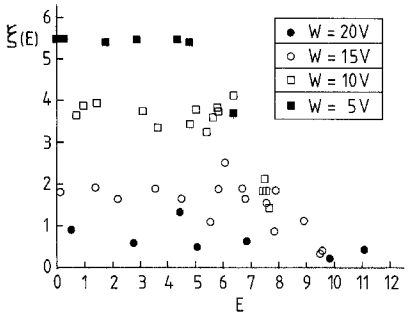

Fig. 11. The localization length $\xi(E)$ of eigenstates of different energies E for $41 \times 41 \times 41$ lattices of various degree of disorder. Note that when $|E|$ becomes larger than the mobility edge value the number of eigenstates, detectable in the simulation, drops to zero. Energy E is in units of the hopping energy V

Figure 11 depicts all our data for the localization length (obtained from the second central moment) of 3D simple cubic lattices, containing 68921 lattice sites, for various degrees of disorder. The most accurate estimate for the critical value of W above which all eigenstates are localized is $W_c \approx 16.5 \pm 0.1$ [53]. Guided by the mobility edge trajectory given in Ref. 16, we investigate the localization properties if one crosses the mobility edge. A technical but important point is that on the $41 \times 41 \times 41$ lattice used, it is not reasonable to assume that one can accommodate localized states for which the localization length is larger than 4, simply because then there is too much probability at the lattice boundary. On the 40-site length scale such states are extended. Thus the data for $W = 5V$ does not allow us to say anything about the nature of the eigenstates. The data for ξ for the case $W = 10V$ suggest that localization sets in if $|E|$ exceeds $7.5V$, a value for $|E|$ which is in good agreement with that given in Ref. 16. Our simulations also show that slightly beyond this point $|E| \approx 8V$, the DOS drops to zero. In other words the range of E in which localized states appear is rather small. For $W = 5V$ it is not detectable at all. For $W = 15V$ no "extended" states have been observed, suggesting that $W_c < 15V$. The fact that this value is lower than the one obtained by the rod technique [21] agrees with the observation made earlier, namely that the strip or rod method over-estimates the localization length. For $W = 20V$ the localization length is of the order of one lattice site, almost independent of $|E|$.

We are grateful to W. Götze, A. Lagendijk, and R. Oppermann for many helpful suggestions and comments. We would like to thank U. Krey and F. Wegner for drawing our attention to an error in the Fourier transform procedure used in the early stage of this work. This work is partially supported by the Belgian National Science Foundation (NFWO) and is part of the research program of the "Stichting voor Fundamenteel Onderzoek der Materie" (FOM), which is financially supported by the "Nederlandse Organisatie voor Wetenschappelijk Onderzoek" (NWO). HDR is senior research associate of the NFWO.

References

1. Thouless, D.J.: Phys. Rep. **13**, 93 (1974)
2. Mott, N.F., Davis, E.A.: Electronic processes in non-crystalline materials. Oxford: Clarendon 1979
3. Nagaoka, Y., Fukayama, H.: Anderson localization. Nagaoka, Y., Fukayama, H. (eds.). Berlin, Heidelberg, New York: Springer 1982
4. Kramer, B., Bergmann, G., Bruynseraede, Y.: Localization, interaction, and transport phenomena. Kramer, B., Bergmann, G., Bruynseraede, Y. (eds.). Berlin, Heidelberg, New York: Springer 1984
5. Lee, P.A., Ramakrishnan, T.V.: Rev. Mod. Phys. **57**, 287 (1985)
6. Möbius, A.: J. Phys.: Condens. Matter **19**, L147 (1986)
7. Wegner, F.: Z. Phys. B – Condensed Matter and Quanta **25**, 327 (1976)
8. Wegner, F.: Z. Phys. B – Condensed Matter and Quanta **35**, 207 (1976)
9. Abrahams, E., Anderson, P.W., Licciardello, D.C., Ramakrishnan, T.V.: Phys. Rev. Lett. **42**, 673 (1979)
10. Anderson, P.W., Thouless, D.J., Abrahams, E., Fisher, D.S.: Phys. Rev. B **22**, 3519 (1980)
11. Götze, W.: Solid State Commun. **27**, 1393 (1978)
12. Götze, W.: J. Phys.: Condens. Matter **12**, 1279 (1979)
13. Götze, W., Prelovšek, P., Wölfle, P.: Solid State Commun. **30**, 369 (1979)
14. Vollhardt, D., Wölfle, P.: Phys. Rev. Lett. **45**, 842 (1980)
15. Vollhardt, D., Wölfle, P.: Phys. Rev. B **22**, 4666 (1980)
16. Zdetsis, A.D.: Soukoulis, C.M., Economou, E.N., Grest, G.S.: Phys. Rev. B **32**, 7811 (1985)
17. Pichard, J.L., Sarma, G.: J. Phys.: Condens. Matter **14**, L127 (1981)
18. MacKinnon, A., Kramer, B.: Phys. Rev. Lett. **47**, 1546 (1981)
19. MacKinnon, A., Kramer, B.: Phys. Rev. Lett. **49**, 695 (1982)
20. MacKinnon, A.: Solid state sciences. Nagaoka, Y., Fukoyama, H. (eds.). Berlin, Heidelberg, New York: Springer 1985
21. MacKinnon, A., Kramer, B.: Z. Phys. B – Condensed Matter **53**, 1 (1983)
22. Economou, E.N., Soukoulis, C.M., Cohen, M.H., Zdetsis, A.D.: Phys. Rev. B **31**, 6172 (1985)
23. Economou, E.N., Soukoulis, C.M., Zdetsis, A.D.: Phys. Rev. B **30**, 1686 (1984)
24. Schönhammer, K., Brenig, W.: Phys. Lett. **42A**, 447 (1973)
25. Prelovšek, P.: Phys. Rev. Lett. **40**, 1596 (1978)
26. Prelovšek, P.: Phys. Rev. B **18**, 3657 (1978)
27. Kramer, B., MacKinnon, A., Weaire, D.: Phys. Rev. B **23**, 6357 (1981)
28. Weaire, D., Srivastava, V.: Amorphous and liquid semiconductors. Spear, W. (ed.). CICL, Univ. of Edinburgh 1977
29. Yoshino, S., Okazaki, M.: J. Phys. Soc. Jpn. **43**, 415 (1977)
30. Lee, P.A.: Phys. Rev. Lett. **42**, 1492 (1979)
31. Ziman, J.M.: Models of disorder. London: Cambridge 1979
32. Stein, J., Krey, U.: Z. Phys. B – Condensed Matter and Quanta **37**, 13 (1980)
33. Scher, H.: Ph.D. thesis Harvard University 1983
34. De Raedt, H.: Comp. Phys. Rep. **7**, 1 (1987)
35. Alben, R., Blume, M., Krakauer, H., Schwartz, L.: Phys. Rev. B **12**, 4090 (1975)
36. MacKinnon, A.: Solid state sciences. Pettifor, D.G., Weaire, D.L. (eds.). Vol. 58. Berlin, Heidelberg, New York: Springer 1985

37. Weaire, D.L.: Solid state sciences. Pettifor, D.G., Weaire, D.L. (eds.), Vol. 58. Berlin, Heidelberg, New York: Springer 1985
38. Weaire, D.L., O'Reilly, E.P.: J. Phys.: Condens. Matter **18**, 1401 (1985)
39. Dwyer, V.M., Weaire, D.L.: Philos. Mag. B **53**, L35 (1986)
40. Anderson, P.W.: Phys. Rev. **109**, 1493 (1958)
41. Vries, P. de, De Raedt, H., Lagendijk, A.: Phys. Rev. Lett. **62**, 2515 (1989)
42. Weaire, D., Williams, A.R.: J. Phys.: Condens. Matter **10**, 1238 (1977)
43. Feit, M.D., Fleck, J.A., Steiger, A.: J. Comp. Phys. **47**, 412 (1982)
44. Wegner, F.: Z. Phys. **44**, 9 (1981)
45. Dean, P.: Rev. Mod. Phys. **44**, 127 (1972)
46. De Raedt, H.: Europhys. Lett. **3**, 139 (1987)
47. Economou, E.N.: Solid state sciences. Vol. 7. Berlin, Heidelberg, New York: Springer 1979
48. Sa-Yakanit, V. Glyde, H.R.: Comm. Condens. Matter Phys. **13**, 35 (1987)
49. Cohen, M.H., Chou, M.Y., Economou, E.N., John, S., Soukoulis, C.M.: IBM J. Res. Dev. **32**, 82 (1988)
50. Halperin, B.I., Lax, M.: Phys. Rev. **148**, 722 (1966)
51. Zittartz, J., Lange, J.S.: Phys. Rev. **148**, 741 (1966)
52. Root, L.J., Bauer, J.D., Skinner, J.L.: Phys. Rev. B **37**, 5518 (1988)
53. Kramer, B.: Anderson localization. Ando, T., Fukuyama, H. (eds.). Berlin, Heidelberg, New York: Springer 1988

Hans De Raedt
Physics Department
University of Antwerp
Universiteitsplein 1
B-2610 Wilrijk
Belgium

P. de Vries
Natuurkundig Laboratorium
University of Amsterdam
Valckenierstraat 65
NL-1018 XE Amsterdam
The Netherlands